

Influence of Atmospheric Rivers on Alaskan River Ice

Russ Limber^{1,2}, Elias Massoud², Jitendra Kumar², Forrest M. Hoffman²

¹The University of Tennessee

²Oak Ridge National Laboratory

Key Points:

- Atmospheric Rivers (ARs) correlate to a one week increase in daily temperature
- Robust ARs occurring during the coldest period of the year appear to prolong the annual breakup date of river ice
- ARs account for about one third (36%) of total precipitation and explain almost half (48%) of interannual variability of precipitation

11 **Abstract**

12 Atmospheric rivers (ARs) transport vast amounts of moisture from low latitudes,
 13 mainly the Tropics, to high latitude regions. One region particularly impacted by ARs
 14 is Alaska USA. We analyze the role of ARs in raising local temperatures, their effect on
 15 precipitation variability, and their influence on the annual river ice breakup date for 25
 16 locations. Precipitation and temperature records were provided by Daymet, with ARs
 17 determined from the Guan and Waliser tracking algorithm. We found ARs increase lo-
 18 cal temperatures for as long as one week post landfall, account for 36% of total precip-
 19 itation and explain 48% of precipitation variability. Calculating the heat transport be-
 20 tween ARs and river ice, fused with a temporal bias, we conclude that heavy precipita-
 21 tion events (HPEs) during the coldest period of the year prolong river ice breakup dates,
 22 while HPEs occurring close to the breakup date have little impact on breakup timing.

23 **Plain language summary**

24 We strategically selected 25 locations with annual river ice breakup dates recorded
 25 throughout Interior Alaska. Across all locations, we determined that daily temperature
 26 increases by up to one week post an atmospheric river (AR). We also found that ARs
 27 account for 36% of total annual precipitation from 1980 to 2023 and explain 48% of the
 28 variability of precipitation. We then calculated the total heat transfer between precip-
 29 itation and river ice while taking into account a bias function for time. Surprisingly, we
 30 found that heavy precipitation events (HPEs), both local precipitation and ARs, that
 31 occur relatively close to river ice breakup dates, have little correlation to the breakup
 32 date. However, HPEs that occur during the coldest period of the year (typically late De-
 33 cember to mid-January) are strongly inversely correlated with river ice breakup timing,
 34 and therefore prolong the breakup date.

35 **1 Introduction**

36 Atmospheric rivers (ARs) are narrow corridors of intense water vapor transport that
 37 significantly influence hydrologic events, transporting most of the water vapor outside
 38 of the Tropics (USDOC, 2023). It is estimated that ARs are responsible for as much as
 39 90% of poleward water vapor transport at midlatitudes (Zhu & Newell, 1998). ARs con-
 40 tribute to extreme precipitation events across various regions worldwide, including West-
 41 ern North America (Dettinger et al., 2004; Neiman et al., 2008; Guan et al., 2010; Paul J.
 42 et al., 2011; Ralph et al., 2006; F. Martin et al., 2019; Dettinger et al., 2011) Europe (Lavers
 43 et al., 2013; Harald & Andreas, 2013), and Western South America (Viale et al., 2018).
 44 In recent years, the impacts of ARs on the cryosphere have been more extensively an-
 45 alyzed. It was found that between 1981 and 2020 atmospheric moisture content anticor-
 46 relates significantly with sea ice concentration over almost the entire Arctic Ocean (Li
 47 et al., 2022). For those same years, another analysis found that 100% of extreme tem-
 48 perature events in the Arctic (above 0 °C) coincides with ARs (Ma et al., 2023). Many
 49 analyses have noted a relationship between heavy AR activity and sea ice loss, caused
 50 by increased rainfall from moisture originating in lower latitudes (Zhang et al., 2023; Maclen-
 51 nan et al., 2022). However Arctic systems are complicated, as the intense moisture trans-
 52 port within ARs can also result in heavy snowfall events, thus contributing to the ac-
 53 cumulation of snowpack, especially in mountainous regions (Saavedra et al., 2020; Guan
 54 et al., 2010). Under the right conditions, this relationship has been found to actually in-
 55 crease the mass balance of glaciers (Little et al., 2019). Understanding the role of ARs
 56 in the cryosphere is essential for assessing their broader impact on regional water resources
 57 and glacier dynamics in a changing climate. While a number of works have explored the
 58 relationship between ARs and sea ice, to our knowledge there haven't been any analy-
 59 ses that look at the relationship between ARs and Arctic river ice. Many works have used
 60 physics based processes and allometrics to model the annual breakup timing and con-

ditions of Arctic river ice (Paily et al., 1974; Ashton, 1986; Prowse et al., 2007; Jasek, 1998; Shen, 2010). While it is recognized that an increase in streamflow alters the dynamics surrounding river ice breakup timing (Ashton, 1986), the relationship precipitation, and to that end AR timing, has on Arctic river ice has yet to be examined. This analysis sets out to answer the following questions: 1.) Is there a change in air temperature for each location corresponding to the timing of ARs? 2.) How do ARs contribute to precipitation throughout interior Alaska? 3.) Do ARs impact the timing of river ice breakup?

2 Data

Similar to previous studies, we define ARs using integrated vapor transport (IVT) values constructed from 6-hourly values of 3-D wind and water vapor at eight pressure levels between 300 and 1,000 mb from the NCEP/NCAR reanalysis data product (Kalnay et al., 1996). AR detection is based on version3 of the tARget algorithm (Guan & Waliser, 2019; Guan, 2022). The IVT values are calculated at the original resolution from the National Center for Environmental Protection (NCEP) meteorological inputs (Saha et al., 2010). AR frequency for a given period within each grid cell is calculated by taking the number of days that detect an AR and dividing by the total number of days in that period. Therefore, for a given grid cell, AR frequency of 0% means there were no AR conditions at any of the time steps and frequency of 100% means there were AR conditions at every time step. Guan and Waliser (Guan & Waliser, 2015) developed a global AR detection algorithm, which was updated and validated later with in situ and dropsonde data (Guan, 2022). This algorithm is employed for our study, which is based on a combination of the IVT magnitude, direction, and geometry characteristics, to objectively identify ARs. Contiguous regions of enhanced IVT transport are first identified from magnitude thresholding (i.e., grid cells with IVT above the seasonally and regionally dependent 85th percentile) and further filtered using directional and geometry criteria requirements. The detection algorithm was applied to NCEP in its native resolution of 2.5°. This detection algorithm had over 90% agreement in detected AR landfall dates with other methods for detecting ARs made for Western North America (Neiman et al., 2008), the United Kingdom (Lavers et al., 2011), and East Antarctica (Gorodetskaya et al., 2014). Precipitation and daily minimum and maximum temperatures (T_{\min} and T_{\max}) were imported from Oak Ridge National Laboratory's Daymet 1kmx1km daily product, via the Distributed Active Archive Center (M. Thornton et al., 2022). River ice breakup dates were collected from the Alaska Pacific River Forecast Center database (APRFC). While exact coordinates were unavailable, coordinates were approximated based on proximity to weather stations and airports to maintain spatial consistency with inputs used in Daymet's meteorological models. 25 locations were identified as having at least 35 breakup records between 1980 and 2023 (the current temporal availability of Daymet). 35 was used as the threshold because it allowed for the greatest number of locations with the most complete time series necessary for statistical analysis.

Daymet precipitation, T_{\min} and T_{\max} were used in our analysis as they have a strong agreement with NCEP temperature outputs for our region of interest Figure 1. Additionally, because Daymet is derived directly from in-situ instruments and meteorological stations, it represents a robust standard for precipitation and temperature predictions across North America (P. E. Thornton et al., 2021).

3 Methods

To determine the impact that ARs have on local temperature, we used a varying temporal window combined with a pairwise t-test. For each AR occurrence, a lookback window and forecast window each equal to n days in length was created before and after the AR date, respectively, whereby: $n \in \{1, 2, 3, \dots, 14\}$. For values of n greater than

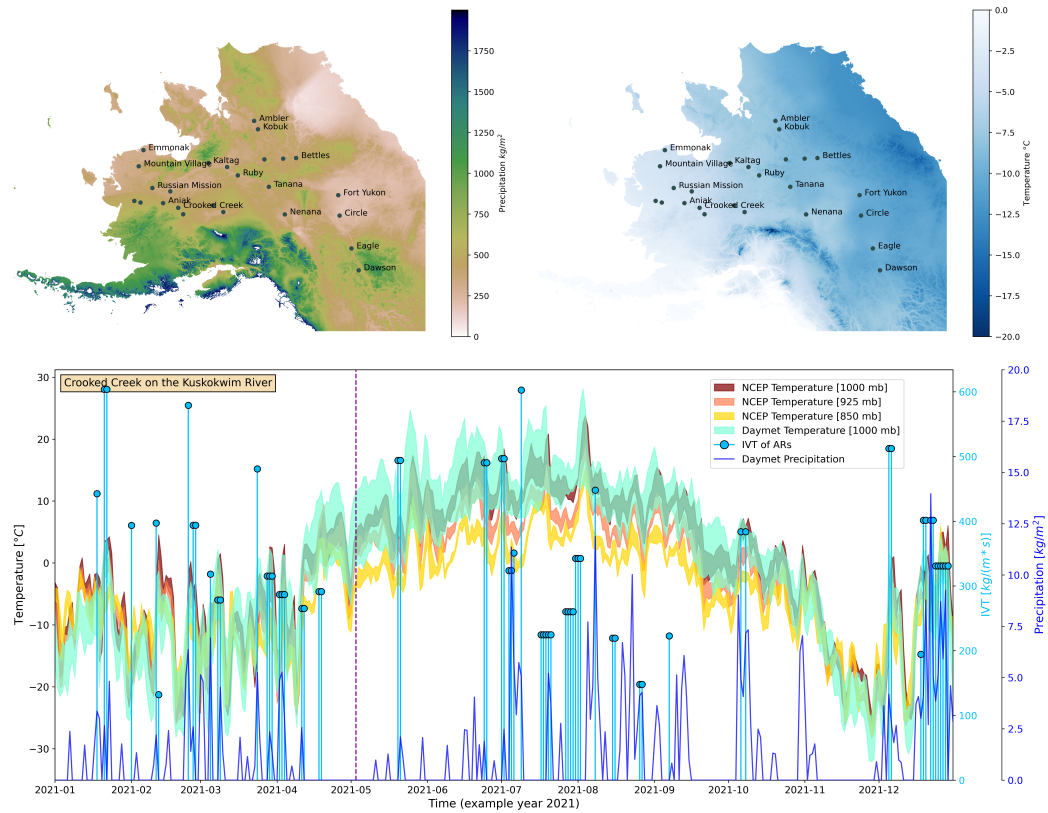


Figure 1. Top: (left) map showing summated precipitation for the year 2021; (right) map of average temperature for 2021. Bottom: One of the 25 locations (Crooked Creek on the Kuskokwim River) for the year 2021. Yellow, orange, red represents the temperature profiles (fill plot of $T_{\min} - T_{\max}$) from NCEP temperature data at 850, 925 and 1000mb respectively. Light green represents Daymet temperature profile. Dark blue shows modeled precipitation from Daymet while the light blue stem plots depict AR events. The purple dashed line shows the breakup date for the Kuskokwim River in 2021 for Crooked Creek.

one day the mean was taken within each window for T_{\min} and T_{\max} . These aggregated temperatures were then calculated over all locations. Aggregated temperature pairs were assessed using a one tailed pairwise t-test to test whether ARs increase local temperature over period of time n ($\alpha = 0.05$). We explored how ARs compare to local precipitation events by separating out precipitation caused by an AR and precipitation not caused by an AR. We then used the Wilcoxon rank-sum test to test the hypothesis that AR events tend to produce more precipitation than local precipitation events (the distributions of precipitation were shown to not be normally distributed even after log transformation using the Shapiro-Wilks test hence the use of a non-parametric test). We calculate the interannual variability of precipitation that ARs account for by conducting a univariate ordinary least squares regression (OLS). To determine the impact that ARs have on river ice breakup timing heat transport was estimated using Equation 1:

$$\frac{dQ}{dt} = \alpha \cdot m \cdot \Delta T \quad (1)$$

where Q is heat flux ($\frac{J}{m^2}$); α specific heat ($\frac{J}{g \cdot ^\circ C}$); ΔT is the difference of ambient temperature and the river ice surface (which is estimated using T_{\min} as a proxy for ambient) ($^\circ C$); m the mass of the precipitation (kg). The integral of these values over all precipitation events that occurred seven months prior to the breakup date is taken with respect to time. A temporal bias function (Equation 2) with tunable parameters is applied to the heat equation to assess when in time precipitation events were more impactful on breakup timing:

$$f(t; \gamma, \kappa, DOY, c) = \begin{cases} \frac{e^{-\gamma \cdot (-t - DOY)} - 1}{\kappa} & \text{if } t < c \\ \frac{e^{-\gamma \cdot (t - DOY)} - 1}{\kappa} & \text{if } t \geq c \end{cases} \quad (2)$$

where γ is a tunable parameter impacting the width of the exponential function; t is time; DOY is the day of year that the breakup date occurred; c is a tunable parameter dictating the center placement of the function κ is a normalizing constant. Finally, Equation 3 is tuned using a full grid search, for each location optimized by the Pearson correlation coefficient.

$$\int_{t_i}^{t_{DOY}} \left(f(t; \gamma, \kappa, DOY, c) \cdot \frac{dQ}{dt} \right) dt \quad (3)$$

4 Results

The pairwise t-test comparing n length lookback and forecast windows found that based on an $\alpha = 0.05$ there is a statistically significant difference in T_{\min} n days prior to an AR event to n days after, when $n \in \{1, \dots, 10\}$ on average. This was true for all locations in the study when $n \in \{1, \dots, 8\}$, at which point the p-values become insignificant for some locations. The t-test for T_{\max} implies that the presence of an AR has less of an effect, with statistical significance found when $n \in \{1, \dots, 6\}$ on average. Some locations showed no significance when $n = 1$ and $n = 6$. Figure 2 shows the change in p-values for each value of n (top row) as well as the mean increase in temperature from the lookback window to the forecast window. The mean temperatures are higher for T_{\min} post AR than T_{\max} , with both plots showing a clear downward trend as the length of n increases.

Figure 3 shows the temporal trends in aggregated IVT and precipitation, over all locations. Interannually, ARs tend to account for 36% of precipitation on average, with a high degree of variability given the year and location (Figure 3 bottom row). The results from the Wilcoxon rank-sum test show that precipitation from ARs tends to be greater

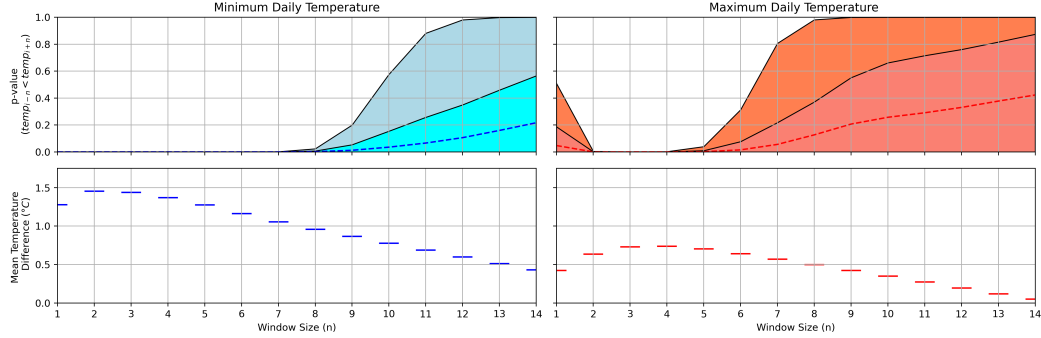


Figure 2. Top: the p-value of the paired t-test given the window size surrounding the AR event date. Dashed lines represent the mean p-value over the study area while the color transition depicts the IQR of p-values Bottom: the average increase in temperature from the lookback window to the forecast window.

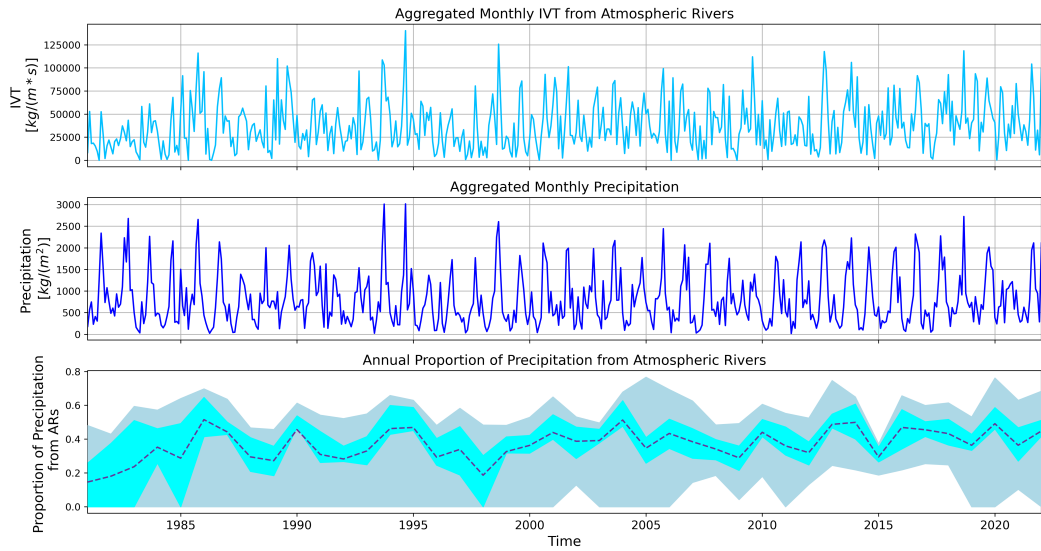


Figure 3. Top: time series of IVT aggregated over all locations. Middle: time series of precipitation aggregated monthly over all locations. Bottom: proportion of precipitation accounted for by ARs, fill colors depict IQR while dashed line depicts the mean, aggregated over all locations annually.

than non-AR precipitation (test statistic = -83.85 ; p-value ≈ 0.0). It was found that of the top 5% of all precipitation events, 57% were caused by ARs (Figure 4 left). Using annual aggregated precipitation from ARs to model total annual aggregated precipitation in a univariate OLS we find that the coefficient of variation (R^2) is equal to 0.48. This means that ARs explain about 48% of interannual variability in precipitation.

Lastly, using Equation 3 to calculate the heat transfer between precipitation and the river ice surface, we note that there is a strong negative correlation between the heat transfer and DOY (Figure 4 upper left) when the bias curve is positioned during the coldest period of the year - typically near January 1st (upper right). In this context, negative values along the y-axis of the left column of the scatterplots are interpreted as a negative heat exchange, meaning a cooling effect on the river ice surface or a deposition

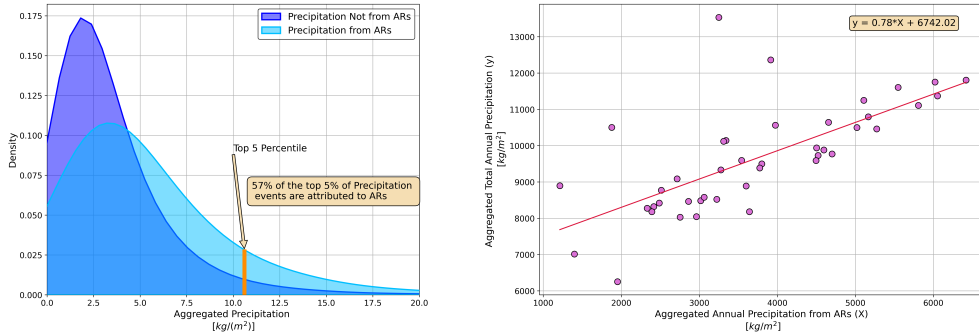


Figure 4. Left: kernel density plots showing the distribution of local precipitation (dark blue) and precipitation from ARs (light blue). Right: ordinary least squares regression plot using annual, summated precipitation from ARs, to predict annual summated precipitation.

of precipitation below freezing. Equation 3 was optimized through adjusting the tunable parameters within the temporal bias (Equation 2) on a location by location basis. For example, Crooked Creek on the Kuskokwim River has a clear negative trend with more robust, colder HPE causing a cooling effect on the river ice surface, prolonging DOY, with a Pearson correlation coefficient (r_p) = -0.84 and a Spearman correlation coefficient (r_s) = -0.80 . The relationship between the total number of ARs that occurred six months prior to the breakup date and the DOY are shown in the center column (top and bottom plots are the same by definition) indicating that the number of ARs prior to river ice breakup appears insufficient in correlating to breakup timing on its own. The bottom row of Figure 5 shows that the use of a bias function is necessary, as simply applying the integral of Equation 1 (the aggregated total heat transfer) is poorly uncorrelated.

5 Conclusion and Discussion

Open research section

This section MUST contain a statement that describes where the data supporting the conclusions can be obtained. Data cannot be listed as "Available from authors" or stored solely in supporting information. Citations to archived data should be included in your reference list. Wiley will publish it as a separate section on the paper's page. Examples and complete information are here: <https://www.agu.org/Publish with AGU/Publish/Author Resources/Data for Authors>

Acknowledgments

Enter acknowledgments here. This section is to acknowledge funding, thank colleagues, enter any secondary affiliations, and so on.

References

- Ashton, G. (1986). *River and lake ice engineering*. Water Resources Publications.
Retrieved from <https://books.google.com/books?id=xg1YVjAsnt8C>
- Dettinger, M. D., Cayan, D. R., Meyer, M. K., & Jeton, A. E. (2004). Simulated hydrologic responses to climate variations and change in the merced, carson, and american river basins, sierra nevada, california, 1900–2099. *Climatic Change*, 62(1), 283–317. Retrieved from <https://doi.org/10.1023/B:CLIM.0000033333.12345>

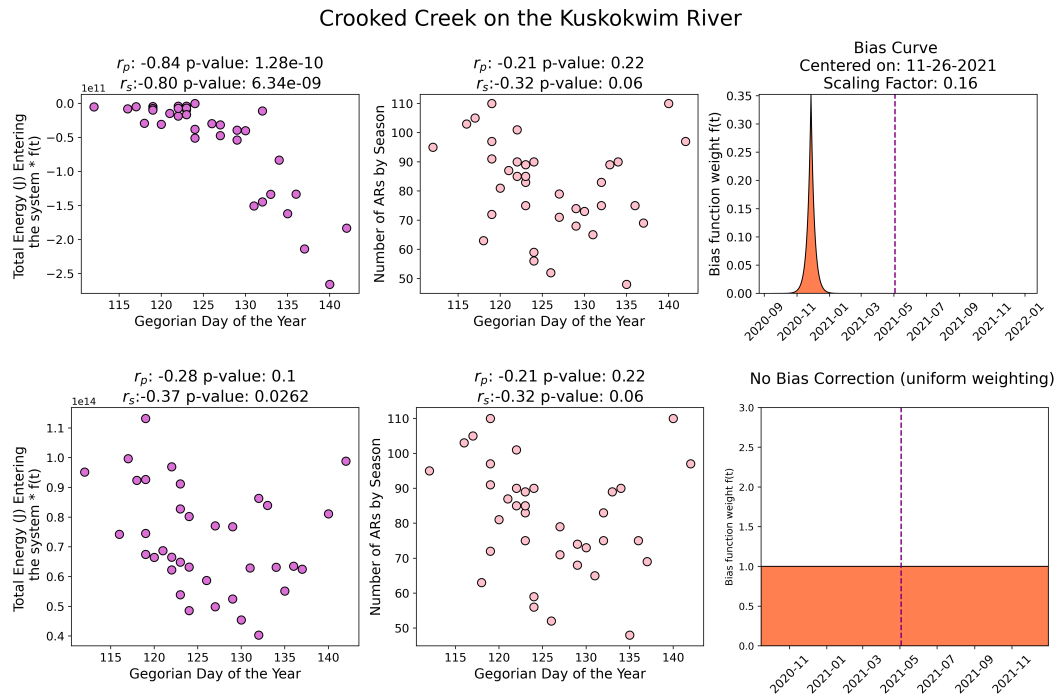


Figure 5. Top: (left) scatter plot between thermal energy transfer and DOY; (middle) scatter plot of the number of ARs that occurred in the six months prior to the breakup date and DOY; (right) temporal bias curve for the year 2021 with the breakup date represented by the vertical dashed line. Bottom: same as the top except depicting the results when a temporal bias is not utilized.

- 191 CLIM.0000013683.13346.4f doi: 10.1023/B:CLIM.0000013683.13346.4f
- 192 Dettinger, M. D., Ralph, F. M., Das, T., Neiman, P. J., & Cayan, D. R. (2011).
 193 Atmospheric rivers, floods and the water resources of California. *Water*, 3(2),
 194 445–478. Retrieved from <https://www.mdpi.com/2073-4441/3/2/445> doi:
 195 10.3390/w3020445
- 196 F. Martin, R., Jonathan J., R., Jason M., C., Michael, D., Michael, A., David, R.,
 197 ... Chris, S. (2019). A scale to characterize the strength and impacts of atmo-
 198 spheric rivers. *Bulletin of the American Meteorological Society*, 100(2), 269 -
 199 289. Retrieved from <https://journals.ametsoc.org/view/journals/bams/100/2/bams-d-18-0023.1.xml> doi: 10.1175/BAMS-D-18-0023.1
- 200 Gorodetskaya, I. V., Tsukernik, M., Claes, K., Ralph, M. F., Neff, W. D., &
 201 Van Lipzig, N. P. M. (2014). The role of atmospheric rivers in anomalous snow
 202 accumulation in east antarctica. *Geophysical Research Letters*, 41(17), 6199-
 203 6206. Retrieved from <https://agupubs.onlinelibrary.wiley.com/doi/abs/10.1002/2014GL060881> doi: <https://doi.org/10.1002/2014GL060881>
- 204 Guan, B. (2022). [Data] Global Atmospheric Rivers Database, Version 3. UCLA
 205 Dataverse. Retrieved from <https://doi.org/10.25346/S6/Y0150N> doi: 10
 206 .25346/S6/Y0150N
- 207 Guan, B., Molotch, N. P., Waliser, D. E., Fetzer, E. J., & Neiman, P. J. (2010).
 208 Extreme snowfall events linked to atmospheric rivers and surface air tem-
 209 perature via satellite measurements. *Geophysical Research Letters*, 37(20).
 210 Retrieved from <https://agupubs.onlinelibrary.wiley.com/doi/abs/10.1029/2010GL044696> doi: <https://doi.org/10.1029/2010GL044696>
- 211 Guan, B., & Waliser, D. (2019, 12). Tracking atmospheric rivers globally: Spat-
 212 tial distributions and temporal evolution of life cycle characteristics. *Journal of*
 213 *Geophysical Research: Atmospheres*, 124. doi: 10.1029/2019JD031205
- 214 Guan, B., & Waliser, D. E. (2015). Detection of atmospheric rivers: Evaluation
 215 and application of an algorithm for global studies. *Journal of Geophysical Re-
 216 search: Atmospheres*, 120(24), 12514-12535. Retrieved from <https://agupubs.onlinelibrary.wiley.com/doi/abs/10.1002/2015JD024257> doi: <https://doi.org/10.1002/2015JD024257>
- 217 Harald, S., & Andreas, S. (2013). Moisture origin and meridional trans-
 218 port in atmospheric rivers and their association with multiple cyclones.
 219 *Monthly Weather Review*, 141(8), 2850 - 2868. Retrieved from <https://journals.ametsoc.org/view/journals/mwre/141/8/mwr-d-12-00256.1.xml>
 220 doi: 10.1175/MWR-D-12-00256.1
- 221 Jasek, M. (1998, July 27–31). 1998 break-up and flood on the yukon river at dawson
 222 – did el niño and climate change play a role? In H. Shen (Ed.), *Ice in surface*
 223 *waters: Proceedings of the 14th international symposium on ice* (pp. 761–768).
 224 Rotterdam: A.A. Balkema.
- 225 Kalnay, E., Kanamitsu, M., Kistler, R., Collins, W., Deaven, D., Gandin, L., ...
 226 Joseph, D. (1996). The ncep/ncar 40-year reanalysis project. *Bulletin*
 227 *of the American Meteorological Society*, 77(3), 437 - 472. Retrieved from
 228 https://journals.ametsoc.org/view/journals/bams/77/3/1520-0477-1996_077_0437_tnyrp_2_0_co_2.xml doi: 10.1175/1520-0477(1996)077(0437:TNYRP)2.0.CO;2
- 229 Lavers, D. A., Allan, R. P., Villarini, G., Lloyd-Hughes, B., Brayshaw, D. J., &
 230 Wade, A. J. (2013). Future changes in atmospheric rivers and their impli-
 231 cations for winter flooding in britain. *Environmental Research Letters*, 8(3).
 232 Retrieved from <https://doi.org/10.1088/1748-9326/8/3/034010> doi:
 233 10.1088/1748-9326/8/3/034010
- 234 Lavers, D. A., Allan, R. P., Wood, E. F., Villarini, G., Brayshaw, D. J., & Wade,
 235 A. J. (2011). Winter floods in britain are connected to atmospheric
 236 rivers. *Geophysical Research Letters*, 38(23). Retrieved from <https://agupubs.onlinelibrary.wiley.com/doi/abs/10.1029/2011GL049783> doi:
 237 10.1029/2011GL049783

- 246 https://doi.org/10.1029/2011GL049783
 247 Li, L., Cannon, F., Mazloff, M. R., Subramanian, A. C., Wilson, A. M., & Ralph,
 248 F. M. (2022). Impact of atmospheric rivers on arctic sea ice variations. *EGU-
 249 sphere, 2022*, 1–21. Retrieved from <https://egusphere.copernicus.org/preprints/2022/egusphere-2022-36/> doi: 10.5194/egusphere-2022-36
 250 Little, K., Kingston, D. G., Cullen, N. J., & Gibson, P. B. (2019). The role of at-
 251 mospheric rivers for extreme ablation and snowfall events in the southern alps
 252 of new zealand. *Geophysical Research Letters, 46*(5), 2761-2771. Retrieved
 253 from <https://agupubs.onlinelibrary.wiley.com/doi/abs/10.1029/2018GL081669> doi: <https://doi.org/10.1029/2018GL081669>
 254 Ma, W., Wang, H., Chen, G., Qian, Y., Baxter, I., Huo, Y., & Seefeldt, M. W.
 255 (2023). Wintertime extreme warming events in the high arctic: Characteristics,
 256 drivers, trends, and the role of atmospheric rivers. *EGUsphere*. Retrieved
 257 from <https://doi.org/10.5194/egusphere-2023-2018> (Preprint) doi:
 258 10.5194/egusphere-2023-2018
 259 Maclennan, M. L., Lenaerts, J. T. M., Shields, C., & Wille, J. D. (2022). Contri-
 260 bution of Atmospheric Rivers to Antarctic Precipitation. *Geophysical Research
 261 Letters, 49*(18). Retrieved 2024-04-16, from <https://onlinelibrary.wiley.com/doi/abs/10.1029/2022GL100585> doi: 10.1029/2022GL100585
 262 Neiman, P. J., Ralph, F. M., Wick, G. A., Kuo, Y.-H., Wee, T.-K., Ma, Z., ... Det-
 263 ttinger, M. D. (2008). Diagnosis of an intense atmospheric river impacting
 264 the pacific northwest: Storm summary and offshore vertical structure observed
 265 with cosmic satellite retrievals. *Monthly Weather Review, 136*(11), 4398 -
 266 4420. Retrieved from <https://journals.ametsoc.org/view/journals/mwre/136/11/2008mwr2550.1.xml> doi: 10.1175/2008MWR2550.1
 267 Paily, P., Macagno, E., & Kennedy, J. (1974, 3). Winter-regime surface heat loss
 268 from heated streams. research report. *US Office of Scientific and Technical In-
 269 formation*. Retrieved from <https://www.osti.gov/biblio/7179276>
 270 Paul J., N., Lawrence J., S., F. Martin, R., Mimi, H., & Gary A., W. (2011).
 271 Flooding in western washington: The connection to atmospheric rivers.
 272 *Journal of Hydrometeorology, 12*(6), 1337 - 1358. Retrieved from https://journals.ametsoc.org/view/journals/hydr/12/6/2011jhm1358_1.xml doi:
 273 10.1175/2011JHM1358.1
 274 Prowse, T., Bonsal, B., Duguay, C., & Lacroix, M. (2007). River-ice break-up/freeze-
 275 up: a review of climatic drivers, historical trends and future predictions. *An-
 276 nals of Glaciology, 46*, 443–451. doi: 10.3189/172756407782871431
 277 Ralph, F. M., Neiman, P. J., Wick, G. A., Gutman, S. I., Dettinger, M. D., Cayan,
 278 D. R., & White, A. B. (2006). Flooding on california's russian river: Role
 279 of atmospheric rivers. *Geophysical Research Letters, 33*(13). Retrieved
 280 from <https://agupubs.onlinelibrary.wiley.com/doi/abs/10.1029/2006GL026689> doi: <https://doi.org/10.1029/2006GL026689>
 281 Saavedra, F., Cortés, G., Viale, M., Margulis, S., & McPhee, J. (2020). At-
 282 mospheric rivers contribution to the snow accumulation over the southern
 283 andes (26.5° s–37.5° s). *Frontiers in Earth Science, 8*. Retrieved from
 284 <https://www.frontiersin.org/articles/10.3389/feart.2020.00261>
 285 doi: 10.3389/feart.2020.00261
 286 Saha, S., Moorthi, S., Pan, H.-L., Wu, X., Wang, J., Nadiga, S., ... Goldberg, M.
 287 (2010). The ncep climate forecast system reanalysis. *Bulletin of the Amer-
 288 ican Meteorological Society, 91*(8), 1015 - 1058. Retrieved from https://journals.ametsoc.org/view/journals/bams/91/8/2010bams3001_1.xml
 289 doi: 10.1175/2010BAMS3001.1
 290 Shen, H. T. (2010). Mathematical modeling of river ice processes. *Cold Re-
 291 gions Science and Technology, 62*(1), 3-13. Retrieved from <https://www.sciencedirect.com/science/article/pii/S0165232X10000339> doi:
 292 <https://doi.org/10.1016/j.coldregions.2010.02.007>

- 301 Thornton, M., Shrestha, R., Wei, Y., Thornton, P., Kao, S.-C., & Wilson, B.
 302 (2022). *Daymet: Annual climate summaries on a 1-km grid for north america,*
 303 *version 4 r1.* ORNL Distributed Active Archive Center. Retrieved
 304 from https://daac.ornl.gov/cgi-bin/dsviewer.pl?ds_id=2130 doi:
 305 10.3334/ORNLDAAAC/2130
- 306 Thornton, P. E., Shrestha, R., Thornton, M., Kao, S.-C., Wei, Y., & Wilson,
 307 B. E. (2021, 7 23). Gridded daily weather data for north america with
 308 comprehensive uncertainty quantification. *Scientific Data*, 8(1), 190. Re-
 309 trieved from <https://doi.org/10.1038/s41597-021-00973-0> doi:
 310 10.1038/s41597-021-00973-0
- 311 USDOC. (2023, 3). *What are atmospheric rivers?* National Oceanic and At-
 312 mospheric Administration. Retrieved from <https://www.noaa.gov/stories/what-are-atmospheric-rivers>
- 313 Viale, M., Valenzuela, R., Garreaud, R. D., & Ralph, F. M. (2018). Impacts
 314 of atmospheric rivers on precipitation in southern south america. *Journal*
 315 *of Hydrometeorology*, 19(10), 1671 - 1687. Retrieved from https://journals.ametsoc.org/view/journals/hydr/19/10/jhm-d-18-0006_1.xml
 316 doi: 10.1175/JHM-D-18-0006.1
- 317 Zhang, P., Chen, G., Ting, M., Ruby Leung, L., Guan, B., & Li, L. (2023, March).
 318 More frequent atmospheric rivers slow the seasonal recovery of arctic sea ice.
 319 *Nature Climate Change*, 13(3), 266–273. Retrieved from <https://doi.org/10.1038/s41558-023-01599-3> doi: 10.1038/s41558-023-01599-3
- 320 Zhu, Y., & Newell, R. E. (1998). A proposed algorithm for moisture fluxes
 321 from atmospheric rivers. *Monthly Weather Review*, 126(3), 725 - 735.
 322 Retrieved from https://journals.ametsoc.org/view/journals/mwre/126/3/1520-0493_1998_126_0725_apafmf_2.0.co_2.xml doi: 10.1175/1520-0493(1998)126<0725:APAFMF>2.0.CO;2
- 323

328 **Appendix A.**